Profiling Blood Lymphocyte Interactions with Cancer Cells Uncovers the Innate Reactivity of Human γδ T Cells to Anaplastic Large Cell Lymphoma[1]

Mary Poupot, Frédéric Pont, and Jean-Jacques Fournié[2]

Quantifying the contacts that circulating lymphocytes have with cancer cells is useful, because their deficit favors malignancy progression. All normal lymphocytes contact, scan, and acquire membrane fragments (trogocytosis) from foreign cells for their immunosurveillance. So in this study, we used the in vitro trogocytosis of PKH67-stained cancer cell lines as a measure of their interactions with bulks of PBMC freshly isolated from healthy donors. Allogeneic PBMC mixed and coincubated in vitro for 1 h did not trogocytosis, whereas in the same conditions CD20$^+$, CD4$^+$, CD8$^+$, γδ T, and CD16$^+$ PBMC interacted strongly with the cancer cells. Although most unprimed lymphoid effectors of innate (NK) and adaptive (B and T) immunity from healthy donors spontaneously trogocytosed different tumoral cell lines, some carcinoma cell lines could escape them in the coculture. This also uncovered the strong interactions of circulating Vγ9/Vδ2$^+$ central memory γδ T cells with anaplastic large cell lymphoma. These interaction profiles were stable upon time for healthy blood donors but were different with other tumors and blood donors. This profiling provides interaction signatures for the immunomonitoring of cancer. *The Journal of Immunology,* **2005, 174: 1717–1722.**

The lack of interactions between cancer cells and lymphoid effectors facilitates malignancy outgrowth, because it may hamper both priming of naive T cells, and activation and response of cytolytic effector cells (1–3). All lymphoid cells initiate their interactions with surveyed cells by settling immunological synapses, which enable their surface receptors to interact with ligands, to concentrate activation signals, and finally to deliver effector functions. The lymphocyte cell surface in this contact area makes small membrane bridges with the target cell (4) and captures patches of its membrane on its own cell surface (5–7), an active process referred to as trogocytosis (8). Because its extent reflects Ag-specific activation of the effector cells (9), the trogocytosis of Tax_{11-19}-HLA-GFP by CD8 αβ T lymphocytes has recently permitted detection and identification of human T cell leukemia virus-specific subsets of CD8 αβ T cells from bulk PBMC in human T cell leukemia virus-infected donors (10). However, in addition to peptide-MHC complex (5, 11), various ectopic molecules stripped from the surface of APC have been detected on effector lymphocyte membranes, including B cell Ag (12), H-2D (13), Igμ (14), and CD21 (15). Because this molecular stripping from APC surfaces is nonselective, nontoxic lipophilic fluorochromes (e.g., PKH26) stably inserted into membranes of target cell or APC were also transferred (11) and could monitor trogocytosis by effector lymphocytes (9). By this approach, the extent of trogocytosis was found related to the activation of functionally mature B, αβ T, γδ T, and NK effector cells by their respective stimulating ligands on Ag/target cell surface (16), and the autoreactive BCR from some lymphoma cell lines induced spontaneous homosynaptic transfers (17).

It is therefore of interest to develop a flow cytometry technique identifying in bulks of PBMC the lymphoid subsets that interacted with cancer cell lines, regardless of their respective immunological response. Because trogocytosis constituted a common readout for contacts by functionally diverse lymphoid effectors, we hypothesized in this study that its measure could undiscriminatively quantify their interactions with cancer cell lines, and so we developed a flow cytometry assay for this purpose.

Materials and Methods

Blood samples and cell lines

Fresh blood samples were collected from healthy EBV$^+$ adult donors, diluted 1/2 in RPMI 1640, centrifuged 1000 × *g* for 10 min on Leucosep tubes (Greiner Bio-One), and the collected PBMC were washed twice for assays. The cell lines Daudi, L428, SUDHL1, CCRF-CEM, P12-Ichikawa, OCI-Ly8, COST, Pio, Karpas-299, K562, THP-1, U937, KG1, Jurkat, DU145, MDA-MB-231, HT29, SW480, NCI-H460, and NCI-H1299 were obtained from American Type Culture Collection and cultured as described (17); the NK92 cell line was provided by E. Vivier (Centre d'Immunologie de Marseille Luminy, Marseilles, France) and was maintained with complete medium supplemented by 50 U/ml IL-2. The ROSK and VAL B lymphoblastoid cell lines were kindly provided by G. Delsol (Institut National de la Santé et de la Recherche Médicale, Unité 563). The pancreas carcinoma cell line Capan-1 was provided by L. Buscail (Centre Hospitalier Universitaire Rangueil) as described above. The carcinoma was cultured in DMEM with 4.5 g/L glucose (BioWhittaker) supplemented with Glutamax-1 and 10% FCS except MDA-MB-231, which was grown in DMEM/NUT MIX (Invitrogen Life Technologies) supplemented as above. Adherent cells were trypsinized for 3 min at 37°C and washed in culture medium before PKH67 labeling. The viability of labeled targets was always >90% in assays.

Staining with fluorochromes and flow cytometry

Cells stained by PKH were coincubated with PBMC in 96-well U-bottom tissue culture plates at a final concentration of 6×10^5 cells in 100 μl of complete RPMI 1640 plus 10% FCS and processed for trogocytosis (17).

Groupe d'Etude des Antigènes Non-Conventionnels, Departement Oncogénèse & Signalisation dans les Cellules Hématopoiétiques, Unité 563 de l'Institut National de la Santé et de la Recherche Médicale, Centre de Physiopathologie de Toulouse Purpan, Boite Postale, Toulouse, France

Received for publication May 17, 2004. Accepted for publication October 19, 2004.

The costs of publication of this article were defrayed in part by the payment of page charges. This article must therefore be hereby marked *advertisement* in accordance with 18 U.S.C. Section 1734 solely to indicate this fact.

[1] This work was supported by institutional funds from Institut National de la Santé et de la Recherche Médicale, Association pour la Recherche sur le Cancer Contract 3283 (to J.-J.F.), and a grant from GIP Aventis (to M.P.).

[2] Address correspondence and reprint requests to Dr. Jean-Jacques Fournié, Departement Oncogénèse & Signalisation dans les Cellules Hématopoiétiques, Unité 563 de l'Institut National de la Santé et de la Recherche Médicale, Centre de Physiopathologie de Toulouse Purpan, Boite Postale 3028, Hôpital Purpan, 31024 Toulouse Cedex 3, France. E-mail address: fournie@toulouse.inserm.fr

Copyright © 2005 by The American Association of Immunologists, Inc.

0022-1767/05/$02.00

The PKH67 mean fluorescence intensity (mfi)[3] values were computed from 10,000–20,000 gated cells in all experiments, and experiments were repeated three to five times. For pretreatment of PKH-labeled cells, these were kept either with anti-Igμ (4 μg/ml, 45 min at 4°C) or control Ig (10 μg/ml), mixed by gentle pelleting, incubated for 1 h at 37°C, and then analyzed by flow cytometry. The specified PBMC subsets were stained for 45 min at 4°C with the following mAbs (1/50 dilution): anti-CD20-PE (blood B lymphocytes), anti-CD16-PE (NK cells), anti-pan TCR $\gamma\delta$-PE ($\gamma\delta$ T lymphocytes), anti-pan TCR $\alpha\beta$-PE ($\alpha\beta$ T lymphocytes), anti-CD4-PE and anti-CD8-PE, goat anti-mouse-PE conjugate (1/50), and isotype controls (5 μg/ml) (Beckman Coulter). Confocal microscopy and ^{51}Cr release assay were described previously (17).

Statistical analysis and graphic representation

The mfi of PKH67 were computed by CellQuest (BD Biosciences). Some distributions were not Gaussian, so their comparison was done by Mann-Whitney rank sum tests using SigmaStat 3.0 (SPSS). The mfi values shown in Fig. 4 were visualized by a graphical color code computed with a software developed in-house and available upon request (⟨frederic.pont@toulouse.inserm.fr⟩). Each mfi value was converted to a gray color scale by linear interpolation from the extreme mfi data, a ppm file in binary format of 256 gray levels was generated, converted to TIFF, and colored by applying a green lookup table.

Results

Spontaneous trogocytosis during short PBMC interaction with tumor cells

We had previously described the ability of primary human $\gamma\delta$ T cell lines to trogocytose Daudi cells in vitro (14). So we used this cell line again to assay similarly the spontaneous interaction with PBMC freshly isolated from healthy donors. Daudi cells stably stained with PKH67 were coincubated for 1 h with unstained PBMC before FACS analysis. Flow cytometry unambiguously discriminated small PBMC from the larger PKH67^{bright} lymphoma cells using forward light scatter/side light scatter or FL1/FL2 dot plots. Comparing the mean intensity of PKH67 fluorescence (below referred to as mfi) on gated PBMC at t0 and t60 min showed an increase upon coculture (Fig. 1*A*). To check that this was trogocytosis of Daudi cell-derived PKH67 by PBMC, we measured acquisition of a transmembrane protein from the lymphoma cell surface. The Igμ of PKH67$^+$ Daudi cells was labeled with specific mouse Ig and secondary PE-conjugated goat anti-mouse Ig, before measuring transfer as above. Neither of the control experiments in which Daudi cells were unlabeled or labeled with controls including isotype-matched Ig, mouse anti-Igμ alone, or isotype Ig plus PE-conjugated anti-isotype did increase the PE fluorescence excluding both Ig-mediated artifacts and uncompensated PKH67 detection in the PE channel. However, PBMC coincubated with the PKH67$^+$ Igμ-PE$^+$ Daudi cells had simultaneously acquired both fluorescences (gate on PBMC only; Fig. 1*B*), demonstrating that PBMC, which acquired PKH67 from tumor cells also received their Igμ transmembrane protein. Confocal microscopy of these tumor cells coincubated for 1 h with PBMC previously stained with Cell Tracker Orange-5-(and -6-)-{[(4-chloromethyl)benzoyl] amino}tetramethylrhodamine (Molecular Probes) confirmed that PBMC in contact with the PKH67$^+$ Daudi were PKH67$^+$ themselves, whereas isolated PBMC were not (Fig. 1, *C* and *D*). Together, these data demonstrated trogocytosis of the Daudi B cell lymphoma cells by a bulk of PBMC shortly coincubated in vitro at 37°C.

Identification of PBMC subsets which trogocytosed Daudi

In the previous experiment, the PBMC were heterogeneously stained by the Daudi cell-derived stain (Fig. 1*B*), suggesting that it was trogocytosed differently by the PBMC subpopulations. So we repeated this experiment and labeled all cells after the coincubation with five subset-specific PE conjugates in parallel assays to compare their respective activity. The markers involved were CD20, CD4, CD8, pan-$\gamma\delta$ TCR, and CD16, used in this study to merely reflect NK cells. Two-color FACS analysis of gated lymphocytes confirmed that these subsets had done trogocytosis of the Daudi cells although with different intensities unrelated to their respective frequency within PBMC. Fifteen percent of PBMC were CD20 cells, which reached a trogocytosis mfi of 14, whereas 52% of PBMC were CD4 cells with mfi = 32, 20% of PBMC were CD8 with mfi = 18, $\gamma\delta$ T cells represented 1% of PBMC and had an mfi = 30, and 19% of PBMC were CD16 cells with mfi = 21 (Fig. 2*A*). Of note, because all the coincubated cells were immunostained and the Daudi lymphoma was CD20$^+$, a minor increase of CD20 expression after 60 min by non-CD20 lymphocytes illustrated further the trogocytosis of this marker (15). This was not observed with the other markers involved here, which were not expressed by Daudi. So both circulating CD4$^+$ and $\gamma\delta$ T lymphocytes from PBMC of donor A interacted with Daudi. This interaction pattern with Daudi was consistently recorded along five successive tests of the same healthy donor (A) over a period of 3 mo (not shown), indicating that it is a stable feature for a defined healthy individual and cancer cell line.

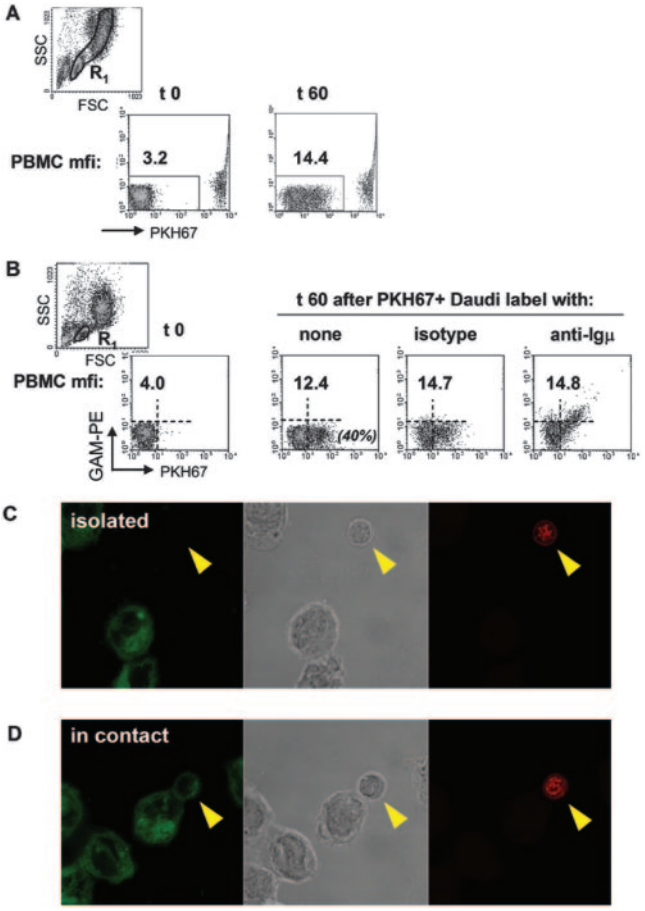

FIGURE 1. Fresh PBMC interact with coincubated Daudi cells by spontaneous trogocytosis. *A*, PKH67 fluorescence of PBMC coincubated for 0 and 60 min with PKH67$^+$ Daudi cells (R_1 gate) in the specified conditions (numbers indicate the PKH67 mfi for boxes). *B*, PBMC acquired both Daudi-derived PKH67 and Igμ (gated in R_1). *C* and *D*, Confocal microscopy (*left panel*, green fluorescence; *middle panel*, transmitted light; *right panel*, red fluorescence) shows that PBMC (Cell Tracker Orange-5-(and -6-)-{[(4-chloromethyl)benzoyl]amino}tetramethylrhodamine$^+$ cells, arrows). PBMC in contact with PKH67$^+$ Daudi cells acquired PKH67, whereas isolated PBMC did not.

[3] Abbreviation used in this paper: mfi, mean fluorescense intensity.

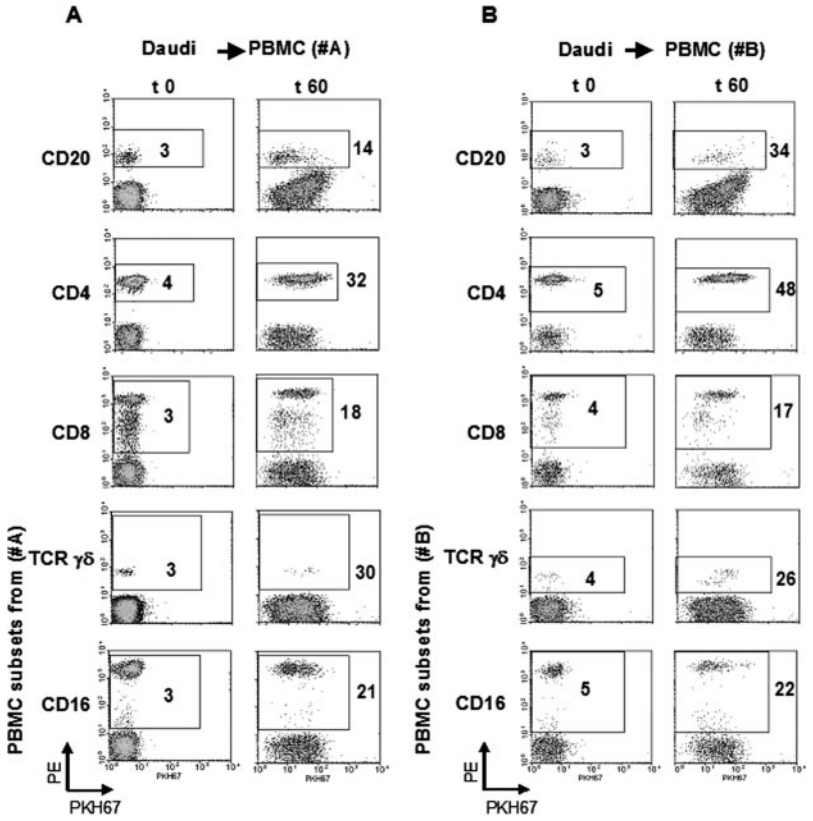

FIGURE 2. PBMC subsets interacting with Daudi. *A*, Differential trogocytosis of Daudi cells by the specified subsets of bulk PBMC from donor A. Each subset was gated using isotype control-PE conjugates (not shown). *B*, Similar experiment with bulk PBMC from donor B (representative experiment).

However, with another healthy EBV^+ donor B, the results differed: its B and CD4 lymphocytes interacted stronger with Daudi than those from donor A ($p < 0.001$ for both pair comparisons, B-to-B and CD4-to-CD4), whereas its CD8, γδ T, and NK subsets scored similarly (Fig. 2*B*). Although the HLA class I deficiency of Daudi cells fails to activate HLA class I-restricted CD8 T lymphocytes (18) but triggers γδ T cells (19), this feature was also expected to activate NK cells. However, circulating NK cells are in resting state and did not trogocytose Daudi spontaneously. With IL-2-activated PBMC from donor A instead of freshly isolated cells, both γδ T and NK cells gave very strong trogocytosis of Daudi (mfi > 100, data not shown). So, this assay quantified the respective interactions of different PBMC subsets with Daudi and identified differences for this phenotype from donor to donor.

Lack of trogocytosis between healthy allogeneic PBMC mixed for 1 h

Because alloreactivity might presumably contribute to the previous results, we mixed allogeneic PBMC freshly collected from different healthy donors and measured trogocytosis after 1 h of coincubation as previously. PBMC from donor C were stained with PKH67 as targets for alloreactive PBMC from donor D. After coincubation, each of the five subsets from donor D was analyzed by flow cytometry for its respective interactions with the allogeneic PBMC. However, none showed any significant increase (a representative result for CD4 cells shown in Fig. 3*A*). Such experiments were repeated with 13 other combinations of mixed allogeneic PBMC derived from other donors and gave similar results (Fig. 3*B*). So healthy alloreactive lymphocytes do not perform trogocytosis within 1 h of coincubation.

Profiling the PBMC interactions with cancer cell lines

We thus asked whether the PBMC subsets from donor A behaved similar to other hemopoietic tumor cell lines, and we analyzed their interaction with a larger panel of cancer cell lines. This panel of 25 cell lines encompassed five B cell lymphoma, four anaplastic large cell lymphoma, four acute T cell lymphoblastic leukemia, one large granular lymphocyte leukemia, one acute myeloid leukemia, two myelomonocytic leukemia, one chronic myeloid leukemia, as well as lung, colon, breast, prostate, and pancreas carcinomas. All cancer cell lines were brightly labeled with PKH67 (mfi > 5000). As similar mfi (mfi = 4–6) for t0 min of the PBMC were recorded with all the targets, we directly compared their mfi at t60 min. For clarity, the data for each PBMC subset and cancer cell were represented by a color table (Fig. 4*A*). The interaction profiles differed with the various tumors. On average with this donor, the B lymphocytes consistently gave the weakest scores, whereas the CD4 T cells were the most interactive, and the three cytolytic subsets (CD8 T, γδ T, and NK) reacted to extents similar to that of the panel taken as a whole. This global view underlined the strong PBMC interactions with hemopoietic cell lines, notably as B cell lymphoma or anaplastic large cell lymphoma, whereas in contrast, carcinoma was relatively ignored. The strongest interactions of fresh NK cells were with K562, an NK cell-activating erythromyeloid cell line (20). With the four non-Hodgkin B cell lymphoma tested, the most interactive PBMC were CD4 T lymphocytes, whereas with the Hodgkin B lymphoma cell line L428, both T and NK cells interacted equally well. Quite strong transfers from anaplastic large cell lymphoma were observed with T CD4, T CD8, and γδ T lymphocytes as exemplified with Karpas-299 (e.g., mfi of 100–150, in three independent experiments). These were the strongest interactions recorded in these studies. Conversely, acute lymphoblastic leukemia gave heterogeneous profiles in terms of subsets and targets. Most T and NK blood cells strongly interacted with Jurkat, but almost no PBMC trogocytosed P12-Ichikawa. Whole PBMC from donor A trogocytosed very weakly most of the carcinoma lines tested here, for instance, the colon SW480 or pancreas Capan-1 cell lines.

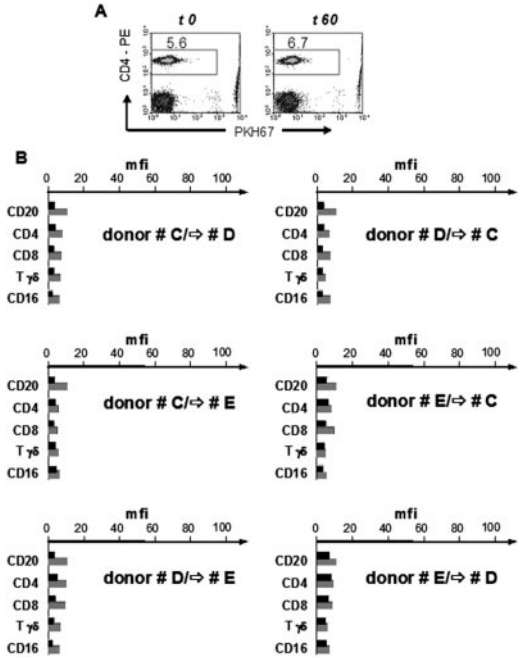

FIGURE 3. Lack of trogocytosis between fresh allogeneic PBMC. *A*, Trogocytosis by $CD4^+$ T cells from donor A PBMC of bulk $PKH67^+$ PBMC from donor B (compare with their activity with Daudi, Fig. 2*A*). *B*, Trogocytosis within six mixed allogeneic PBMC coincubations. Donor C and D, trogocytosis by PBMC from donor D of $PKH67^+$ PBMC from donor C. ■, PKH67 mfi t0 min; ▨, PKH67 mfi t60 min.

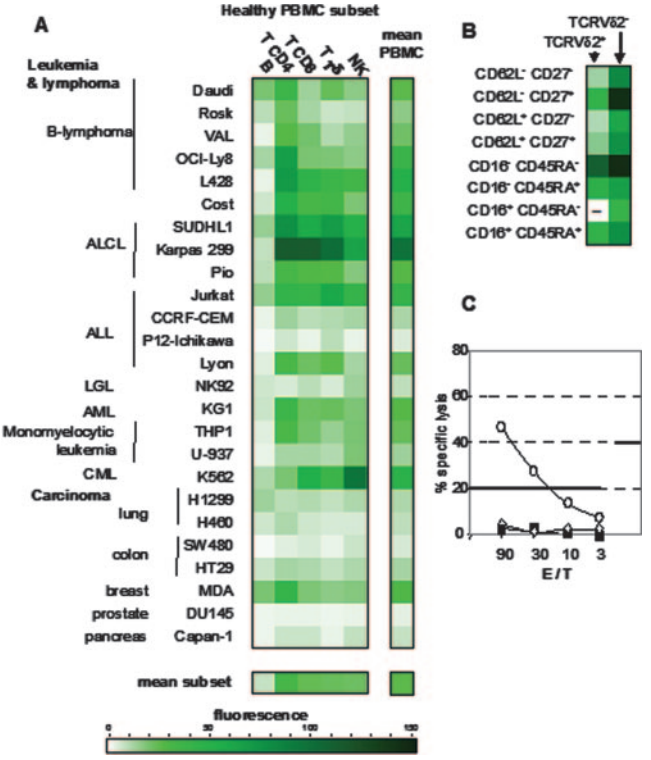

FIGURE 4. Profiling interactions of fresh PBMC with cancer cell lines. *A*, The specified $PKH67^+$ cancer cell lines were tested with bulk PBMC from donor A before measuring the subset-specific interactions as above. γδ T lymphocytes interacting with Karpas-299. *B*, Subtyping of the bulk PBMC interacting with Karpas-299 cells ex vivo (−, not detected). *C*, Fresh PBMC from donor A did not kill Karpas-299 cells (■) nor P12-Ichikawa cells (◇) but lysed K562 targets (○) in a 4-h ^{51}Cr release assay.

γδ T cell interactions with anaplastic large cell lymphoma Karpas-299

The ability of blood γδ T cells to spontaneously interact with anaplastic large cell lymphoma cell lines such as Karpas-299 was previously unknown, so we refined this observation with another set of cell markers. The γδ T cells represented 0.8% of PBMC in donor A, had a $CD4^-CD8^-$ phenotype, and essentially expressed $V\gamma9V\delta2$ TCR^+ lymphocytes (>90% of γδ T cells, data not shown). These cells comprised naive and memory γδ T lymphocytes, as defined by CD45RA, CD27, CD62L, and CD16 markers (21, 22). Freshly collected PBMC from donor A were thus subtyped by two parallel combinations of triple stainings for TCRVδ2/CD16/CD45RA and TCRVδ2/CD27/CD62L. Each of the resulting subsets was then scored for its respective interactions with Karpas-299 through analysis of 100,000 events due to their low frequency in PBMC (~0.1%). The most active subset of $TCRV\delta2^+$ cells were $CD16^-CD45RA^-$ and $CD62L^-CD27^+$ central memory γδ T cells (21, 22). With $TCRV\delta2^-$ PBMC as well, the strongest interactions with Karpas-299 were also mediated by central memory cells (Fig. 4*B*), which were expected to lack cytolytic activity (22). Accordingly, ^{51}Cr-pulsed Karpas-299 cells were not killed by bulk PBMC freshly collected from donor A (compared with the killed target K562 and not killed Ichikawa control; Fig. 4*C*). These results suggested that the reactive central memory γδ T cells were able to efficiently bind anaplastic large cell lymphoma but not to kill them. By contrast, mature cytolytic T lymphocytes obtained by PBMC (same donor) culture with IL-2 strongly trogocytosed and killed Karpas-299 (not shown) after formation of very transient synapses (23). So the γδ PBMC that spontaneously mediated nonlytic trogocytosis of the Karpas-299 cells comprised functionally immature central memory precursors of cytolytic γδ T lymphocytes.

Discussion

This study monitored cell-cell interactions ex vivo between fresh PBMC subsets obtained from healthy donors and established cancer cell lines. The results showed that trogocytosis reflected early cell-to-cell contacts and was favored by stimulatory cell targets. However, as a prerequisite to delivery of effector functions, trogocytosis was not predictive of their functional outcomes. So because it was dissociated from these functional responses, trogocytosis also appeared as a versatile readout for interactions of broadly diverse lymphoid effector cells. This evidenced phenotypes that clearly differed within individuals and cancer cells, and permitted comparison of the cancer cell engagement by B and T cells, which would otherwise need qualitatively different assays. Because, as such, this assay does not identify the functional outcome of these interactions, whether the lymphocytes that trogocytosed had undergone further proliferative, cytolytic, or cytokine responses could not be directly determined at the single-cell level. We now seek to address this issue using different experimental settings and longer cocultures. However, as illustrated with circulating γδ T lymphocytes, this assay enabled the selective monitoring of quantitatively minor, but functionally significant, lymphoid subsets from bulks of PBMC, without need for their physical separation.

The coincubation favored a rapid trogocytosis of some cancer cells by unsensitized PBMC. Although the donor's EBV^+ status could account for trogocytosis of the EBV^+ cancer cells by low frequency EBV-specific B and T PBMC, trogocytosis was instead mediated by whole B or T cell subpopulations, reflecting rather Ag-independent immunological synapses. Lymphoid cells from innate and adaptive immunity make synapses and trogocytosis in

the absence of specific Ag and HLA restriction (14, 15, 24–27). With tumor cell lines activating NK, such as the K562 chronic myeloid erythroleukemia though, this followed the strong recruitment and engagement of stimulatory receptors such as NKG2D or of other broadly distributed activating receptors (28–30). Expression of protective HLA class I molecules by tumoral cells controls their trogocytosis by regulating activation of all NK cells and of the inhibitory NK receptor-positive fraction of γδ T cells (14, 15, 19). Accordingly, the stable β_2-microglobulin-positive transfectant of Daudi was less trogocytosed than the parental Daudi cell line by NK cells from donor A (mfi of 21 with Daudi vs mfi of 12 with Daudi HLA class I^+), whereas the opposite was found with CD8 T lymphocytes from the same donor (mfi of 18 with Daudi vs mfi of 41 with Daudi HLA class I^+ not shown), and no difference was noticed with Vγ9/Vδ2 T lymphocytes, which were essentially negative for inhibitory NK receptors in this donor. Circulating γδ T cells, which recognize a broad set of lymphoid and nonlymphoid malignancies (31) interacted here with most leukemia, although less efficiently with some untouched carcinoma, in agreement with a recent in vivo study (32). Carcinoma-reactive γδ T cells represent few γδ cells in blood, because these usually express Vδ1 TCR and reside rather in epithelia (33).

The majority of blood γδ T cells express Vγ9/Vδ2 and their broad antitumoral activity is well established and of clinical significance for cancer immunotherapies (34–37). This report showed that they could also be of interest against large anaplastic lymphoma, because they strongly trogocytosed several cell lines of this peculiar histotype without known previous exposure of the blood donor. Central memory-type Vγ9/Vδ2 T lymphocytes mostly lack immediate effector functions (21, 22). However, their innate ability to interact strongly with Karpas-299 cells is of interest for large anaplastic lymphoma immunotherapy because they represent an abundant PBMC subset that proliferates strongly and matures into fully functional Th1-type and cytotoxic effector cells upon activation (22, 38). We recovered this innate property with circulating γδ T cells from several healthy donors, warranting an analysis extended to circulating γδ T from large anaplastic lymphoma patients undergoing chemotherapy (our manuscript in preparation). In addition, this new analytical technique will enable monitoring of the attack of cancer cells by blood γδ T cells selectively stimulated in vivo along current clinical trials of γδ T cell-targeted cancer immunotherapies by synthetic phosphoantigen (36) and therapeutic aminobisphosphonates (34, 37).

Although in vitro cell contacts between cancer cells and lymphocytes formally demonstrated that the latter could bind the tumor cells upon exposure, some cell lines, however, could not be caught by normal PBMC in vitro. In more physiopathological conditions, this failure would probably mean immunoevasion and outgrowth of the tumor (3). Because the natural selection of cancer cell variants that escape to lymphocytes through loss of surface ligands generates immunoresistant tumors (39), it is important to determine rapidly whether the PBMC from cancer patients are able to catch their own tumor cells through a straightforward in vitro test. As seen during this study, this phenotype was stable upon time for a healthy individual. This might differ in vivo with tumors under evolutive pressure, warranting an answer to this issue in autologous contexts of cancer patients. Finally, individual PBMC interaction profilings constitute unique signatures of immunosurveillance of cancer cells, which may help in monitoring the specific situations of each patient.

Acknowledgments

We acknowledge G. Delsol, F. Meggetto, J. Selves, A. Quillet-Mary, P. Cordelier, L. Buscail, and E. Vivier for providing cell lines involved in this study, S. Muller for support in confocal microscopy, and Sanofi-Synthélabo (Labège, France) for generous supply of human IL-2. We thank P. Brousset, M. Bonneville, and P. Bousso for stimulating discussions, and M. Allouche and G. Laurent for critical advice for the manuscript.

References

1. Pardoll, D. 2003. Does the immune system see tumors as foreign or self? *Annu. Rev. Immunol. 21:807*.
2. Yu, P., Y. Lee, W. Liu, R. K. Chin, J. Wang, Y. Wang, A. Schietinger, M. Philip, H. Schreiber, and Y. X. Fu. 2004. Priming of naive T cells inside tumors leads to eradication of established tumors. *Nat. Immunol. 5:141*.
3. Ochsenbein, A. F., P. Klenerman, U. Karrer, B. Ludewig, M. Pericin, H. Hengartner, and R. M. Zinkernagel. 1999. Immune surveillance against a solid tumor fails because of immunological ignorance. *Proc. Natl. Acad. Sci. USA 96:2233*.
4. Stinchcombe, J. C., G. Bossi, S. Booth, and G. M. Griffiths. 2001. The immunological synapse of CTL contains a secretory domain and membrane bridges. *Immunity 15:751*.
5. Huang, J. F., Y. Yang, H. Sepulveda, W. Shi, I. Hwang, P. A. Peterson, M. R. Jackson, J. Sprent, and Z. Cai. 1999. TCR-mediated internalization of peptide-MHC complexes acquired by T cells. *Science 286:952*.
6. Hwang, I., J. F. Huang, H. Kishimoto, A. Brunmark, P. A. Peterson, M. R. Jackson, C. D. Surh, Z. Cai, and J. Sprent. 2000. T cells can use either T cell receptor or CD28 receptors to absorb and internalize cell surface molecules derived from antigen-presenting cells. *J. Exp. Med. 191:1137*.
7. Hudrisier, D., and P. Bongrand. 2002. Intercellular transfer of antigen-presenting cell determinants onto T cells: molecular mechanisms and biological significance. *FASEB J. 16:477*.
8. Joly, E., and D. Hudrisier. 2003. What is trogocytosis and what is its purpose? *Nat. Immunol. 4:815*.
9. Hudrisier, D., J. Riond, H. Mazarguil, J. E. Gairin, and E. Joly. 2001. Cutting edge: CTLs rapidly capture membrane fragments from target cells in a TCR signaling-dependent manner. *J. Immunol. 166:3645*.
10. Tomaru, U., Y. Yamano, M. Nagai, D. Maric, P. T. Kaumaya, W. Biddison, and S. Jacobson. 2003. Detection of virus-specific T cells and $CD8^+$ T-cell epitopes by acquisition of peptide-HLA-GFP complexes: analysis of T-cell phenotype and function in chronic viral infections. *Nat. Med. 9:469*.
11. Patel, D. M., P. Y. Arnold, G. A. White, J. P. Nardella, and M. D. Mannie. 1999. Class II MHC/peptide complexes are released from APC and are acquired by T cell responders during specific antigen recognition. *J. Immunol. 163:5201*.
12. Batista, F. D., D. Iber, and M. S. Neuberger. 2001. B cells acquire antigen from target cells after synapse formation. *Nature 411:489*.
13. Zimmer, J., V. Ioannidis, and W. Held. 2001. H-2D ligand expression by $Ly49A^+$ natural killer (NK) cells precludes ligand uptake from environmental cells: implications for NK cell function. *J. Exp. Med. 194:1531*.
14. Espinosa, E., J. Tabiasco, D. Hudrisier, and J. J. Fournie. 2002. Synaptic transfer by human γδ T cells stimulated with soluble or cellular antigens. *J. Immunol. 168:6336*.
15. Tabiasco, J., A. Vercellone, F. Meggetto, D. Hudrisier, P. Brousset, and J. J. Fournie. 2003. Acquisition of viral receptor by NK cells through immunological synapse. *J. Immunol. 170:5993*.
16. Davis, D. M. 2002. Assembly of the immunological synapse for T cells and NK cells. *Trends Immunol. 23:356*.
17. Poupot, M., and J. J. Fournie. 2003. Spontaneous membrane transfer through homotypic synapses between lymphoma cells. *J. Immunol. 171:2517*.
18. Pothen, S., T. Cao, R. Smith, P. H. Levine, A. Levine, and G. R. Pearson. 1993. Identification of T- and B-cell epitopes associated with a restricted component of the Epstein-Barr virus-induced early antigen complex. *Int. J. Cancer 53:199*.
19. Fisch, P., E. Meuer, D. Pende, S. Rothenfusser, O. Viale, S. Kock, S. Ferrone, D. Fradelizi, G. Klein, L. Moretta, et al. 1997. Control of B cell lymphoma recognition via natural killer inhibitory receptors implies a role for human Vγ9/Vδ2 T cells in tumor immunity. *Eur. J. Immunol. 27:3368*.
20. Ortaldo, J. R., G. D. Bonnard, and R. B. Herberman. 1977. Cytotoxic reactivity of human lymphocytes cultured in vitro. *J. Immunol. 119:1351*.
21. Gioia, C., C. Agrati, R. Casetti, C. Cairo, G. Borsellino, L. Battistini, G. Mancino, D. Goletti, V. Colizzi, L. P. Pucillo, and F. Poccia. 2002. Lack of $CD27^-CD45RA^-V\gamma9V\delta2^+$ T cell effectors in immunocompromised hosts and during active pulmonary tuberculosis. *J. Immunol. 168:1484*.
22. Dieli, F., F. Poccia, M. Lipp, G. Sireci, N. Caccamo, C. Di Sano, and A. Salerno. 2003. Differentiation of effector/memory Vδ2 T cells and migratory routes in lymph nodes or inflammatory sites. *J. Exp. Med. 198:391*.
23. Faroudi, M., C. Utzny, M. Salio, V. Cerundolo, M. Guiraud, S. Muller, and S. Valitutti. 2003. Lytic versus stimulatory synapse in cytotoxic T lymphocyte/target cell interaction: manifestation of a dual activation threshold. *Proc. Natl. Acad. Sci. USA 100:14145*.
24. Revy, P., M. Sospedra, B. Barbour, and A. Trautmann. 2001. Functional antigen-independent synapses formed between T cells and dendritic cells. *Nat. Immunol. 2:925*.
25. Sjostrom, A., M. Eriksson, C. Cerboni, M. H. Johansson, C. L. Sentman, K. Karre, and P. Hoglund. 2001. Acquisition of external major histocompatibility complex class I molecules by natural killer cells expressing inhibitory Ly49 receptors. *J. Exp. Med. 194:1519*.
26. McCann, F. E., B. Vanherberghen, K. Eleme, L. M. Carlin, R. J. Newsam, D. Goulding, and D. M. Davis. 2003. The size of the synaptic cleft and distinct distributions of filamentous actin, ezrin, CD43, and CD45 at activating and inhibitory human NK cell immune synapses. *J. Immunol. 170:2862*.

27. Tabiasco, J., E. Espinosa, D. Hudrisier, E. Joly, J. J. Fournie, and A. Vercellone. 2002. Active *trans*-synaptic capture of membrane fragments by natural killer cells. *Eur. J. Immunol. 32:1502*.
28. Pende, D., C. Cantoni, P. Rivera, M. Vitale, R. Castriconi, S. Marcenaro, M. Nanni, R. Biassoni, C. Bottino, A. Moretta, and L. Moretta. 2001. Role of NKG2D in tumor cell lysis mediated by human NK cells: cooperation with natural cytotoxicity receptors and capability of recognizing tumors of nonepithelial origin. *Eur. J. Immunol. 31:1076*.
29. Sutherland, C. L., N. J. Chalupny, and D. Cosman. 2001. The UL16-binding proteins, a novel family of MHC class I-related ligands for NKG2D, activate natural killer cell functions. *Immunol. Rev. 181:185*.
30. Favier, B., E. Espinosa, J. Tabiasco, C. Dos Santos, M. Bonneville, S. Valitutti, and J. J. Fournie. 2003. Uncoupling between immunological synapse formation and functional outcome in human γδ T lymphocytes. *J. Immunol. 171:5027*.
31. Moris, A., S. Rothenfusser, E. Meuer, R. Hangretinger, and P. Fisch. 1999. Role of γδ T cells in tumor immunity and their control by NK receptors. *Microbes Infect. 1:227*.
32. Lozupone, F., D. Pende, V. L. Burgio, C. Castelli, M. Spada, M. Venditti, F. Luciani, L. Lugini, C. Federici, C. Ramoni, et al. 2004. Effect of human natural killer and γδ T cells on the growth of human autologous melanoma xenografts in SCID mice. *Cancer Res. 64:378*.
33. Groh, V., R. Rhinehart, H. Secrist, S. Bauer, K. H. Grabstein, and T. Spies. 1999. Broad tumor-associated expression and recognition by tumor-derived γδ T cells of MICA and MICB. *Proc. Natl. Acad. Sci. USA 96:6879*.
34. Kunzmann, V., E. Bauer, J. Feurle, F. Weissinger, H. P. Tony, and M. Wilhelm. 2000. Stimulation of γδ T cells by aminobisphosphonates and induction of antiplasma cell activity in multiple myeloma. *Blood 96:384*.
35. Kato, Y., Y. Tanaka, H. Tanaka, S. Yamashita, and N. Minato. 2003. Requirement of species-specific interactions for the activation of human γδ T cells by pamidronate. *J. Immunol. 170:3608*.
36. Sicard, H., T. Al Saati, G. Delsol, and J. J. Fournie. 2001. Synthetic phosphoantigens enhance human Vγ9Vδ2 T lymphocytes killing of non-Hodgkin's B lymphoma. *Mol. Med. 7:711*.
37. Wilhelm, M., V. Kunzmann, S. Eckstein, P. Reimer, F. Weissinger, T. Ruediger, and H. P. Tony. 2003. γδ T cells for immune therapy of patients with lymphoid malignancies. *Blood 102:200*.
38. Angelini, D. F., G. Borsellino, M. Poupot, A. Diamantini, R. Poupot, G. Bernardi, F. Poccia, J. J. Fournie, and L. Battistini. 2004. FcγRIII discriminates between two subsets of Vγ9Vδ2 effector cells with different responses and activation pathways. *Blood 104:1801*.
39. Khong, H. T., and N. P. Restifo. 2002. Natural selection of tumor variants in the generation of "tumor escape" phenotypes. *Nat. Immunol. 3:999*.